Phase transformation in Ba -Ti substituted lithium ferrites and subsequent dielectric variations

P.G. BHATIA
Guru Nanak College of Arts, Science and Commerce, GTB Nagar,
Mumbai 400037, pushpindergb@gmail.com[1]

Abstract

Pseudobrookite Fe_2TiO_5 was reduced to a spinel by substituting Fe^{2+} by Li^{+} & Ti^{4+} by Ba^{2+} and the role of Ba^{2+}, Ti^{4+} on the oxide samples was studied. Spinel samples, $Li_{0.9}Fe_{1.1}Ba_{0.1}Ti_{0.9}O_4$ (SP1) and $Li_{0.7}Fe_{1.3}Ba_{0.3}Ti_{0.7}O_4$ (SP2) were prepared by the solid state reaction method. The single phase spinel structure was confirmed using XRD technique and lattice constants were determined. With the increase in Barium content, the symmetry was seen to undergo a change from cubic to tetragonal phase. The cation distribution in the samples was determined. Ba was seen to show a strong preference for the tetrahedral (A) sites. The dielectric constant was measured by varying frequency from 1 Khz to 1 Mhz and in the temperature range from 300^{o}K to 773^{o}K. The tetragonal spinel was observed to show a huge dielectric constant as compared to the cubic spinel. The enhanced dielectric constant makes it a promising battery material and could be studied against the backdrop of phase transformation.

Keywords: Spinel, cation distribution, hysteresis.

Introduction

Ferrites show remarkable electric, magnetic and optical properties making them useful in electronic digital and microwave devices [1], [2], [3], [4]. A number of researchers and engineers are involved in basic studies, improvement, measurement and application of ferrites. Attention is being paid to the crystal structure, magnetic ordering, saturation magnetization and preference of metallic ions for interstitial sites in the spinel lattice [5].

Spinels are mixed metal oxides represented by the formula AB_2O_4 where A and B are metal ions surrounded by oxygen tetrahedral and octahedral respectively. The physical properties of spinels depend upon the composition and cationic arrangement of the molecules present [5]. Spinel ferrites have been established as magnetic materials which occupy smaller volume, have low production cost and are easier to manufacture using ceramic technology.

The unit cell of a spinel lattice consists of 8 molecules with 32 Oxygen ions, 64A-sites and 32B-sites.Out of these, 8A-sites and 16B-sites are filled. The ability of the spinel to distribute cations in these sites in different manners, gives rise to varied physical and chemical properties. The cation distribution is of great importance as the magnetic and electrical nature also depend upon ionic partition among ions; e.g. the magnetic behaviour stems from a strong anti-ferromagnetic coupling of the super-exchange type between magnetic ions on the neighbouring A and B sites; while a weaker coupling takes place between

ions on like sites [6], [7]**.** Therefore, the control of cation distribution provides a means to control magnetic behaviour.

Also, the electrical conductivity and catalytic features depend upon ionic arrangement. In the present work it is thought interesting to investigate the role of Li^{+}, Ba^{2+}, Fe^{3+}, and Ti^{4+} in a spinel by reducing a pseudobrookite to a spinel using the formula $(Li_{x}\ Fe_{2-x})\ (Ba_{y}\ Ti_{1-y})O_4$ where x+y =1, with a view to combining different properties which these cations impart in different environment. Fe^{3+} and Ti^{4+} in a pseudobrookite environment of Fe_2TiO_5 is a good a passive resistive material [8] and is also responsible for microcracking. The choice of Li^{+} and Fe^{3+} rests on their tendency to form a soft magnetic spinel viz. $LiFe_5O_8$ [9]. On the other hand, Ba^{2+} and Fe^{3+} form a hard ferrite viz; $BaFe_{12}O_{19}$ which is a complex perovskite. Ba^{2+} and Ti^{4+} in a perovskite like $BaTiO_3$ render it ferroelectric nature [10]. Of the several combinations, two single phase spinels, viz. $Li_{0.9}Fe_{1.1}Ba_{0.1}Ti_{0.9}O_4$ (SP1) and $Li_{0.7}Fe_{1.3}\ Ba_{0.3}Ti_{0.7}O_4$ (SP2) are formed and their structural, electrical and magnetic behaviour are reported here.

Experimental

Two spinel samples, $Li_{0.9}Fe_{1.1}Ba_{0.1}Ti_{0.9}O_4$ (SP1) and $Li_{0.7}Fe_{1.3}\ Ba_{0.3}Ti_{0.7}O_4$ (SP2) were prepared by the high temperature solid state reaction. The starting materials, Li_2CO_3, Fe_2O_3, TiO_2 and $BaCO_3$ (all 99.9 per cent purity – AR grade) were dried in a muffle furnace at 200^{o}C for 2 hours. These were mixed in stoichiometric proportion, ground and calcined in steps of 600^{o}C, 800^{o}C and 1000^{o}C for eight hours each .To obtain homogeneity, these mixtures were pressed into pellets and were finally sintered for 24 hours at 1200^{o}C to ensure a complete reaction. The crystallographic structure was determined at room temperature using the X-ray diffraction patterns of powders obtained by using a highly sophisticated microprocessor based JEOL-JDX8030 diffractometer using a Copper target. The variation in capacitance C and loss factor tan∂ with frequency in the range 10khz-1Mhz at room temperature was recorded on a HP 4277 A LCZ Meter using a two probe method. The same two probe method system was used to determine dielectric constant, loss and resistivity in the temperature range 300-773K. The Scanning Electron Microscope (SEM) images were obtained from JEOL, JSM-840A/WDS/EDS analytical scanning microscope along with ion sputter JFC-1100. The grain size was determined by the line intercept method [11].

Results and Discussion

Structural investigation: X-Ray Diffraction patterns shown in *Figure I(a) and I(b)* indicate the single phase spinel formation belonging to $LiFe_5O_8$ group . However, SP1 is cubic and SP2 exhibits tetragonal symmetry *(Table I)*. It is interesting to observe that the intensities corresponding to planes (221), (320) and (510) are those corresponding to lithium ferrite (jcpds no: 17011). Moreover, the intensities of all these lines nearly double in SP2 wrt. SP1. The presence of increased quantity of barium, whose ionic radius and atomic number are much larger than the other cations, in these planes could be the cause.

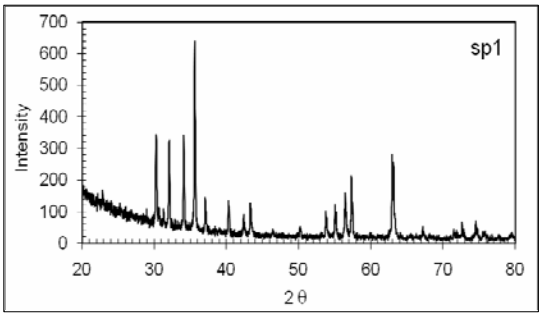

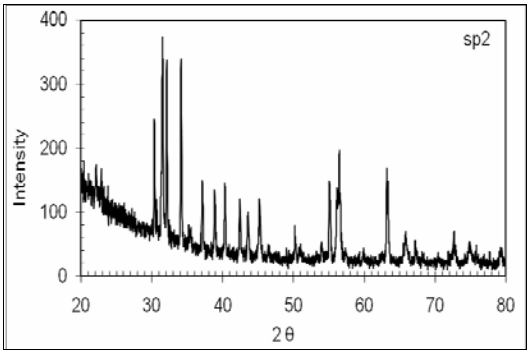

Fig. I (a): X-ray diffraction pattern of SP1

Fig. I(b): X-ray diffraction pattern of SP2

The XRD related material growth parameters are listed in Table I.

TABLE I X-RAY PARAMETERS

	SP1 $Li_{0.9}Fe_{1.1}Ba_{0.1}Ti_{0.9}O_4$	**SP2** $Li_{0.7}Fe_{1.3}Ba_{0.3}Ti_{0.7}O_4$
Lattice const. a=b A^0	a = 8.340	a = 8.304 c = 8.496
Unit cell volume cm^3	580	586
Av. Debye particle size A^0	389	680
Grain size (SEM)	16 µm.	12 µm
Density gm/cc (exptal)	4.29	4.91
Density gm/cc (XRD)	4.753	5.46
Pore fraction	0.37	0.47
Inhomogeneity	0.0021	0.01687

The tetragonality, and larger unit cell size, densities, particle size as well as pore fraction corresponding to SP2 are clearly due to the presence of Barium which has much larger ionic radius and atomic mass than that of other cations.

The *table I* also includes the grain size as determined from SEM. *(Fig.II)*

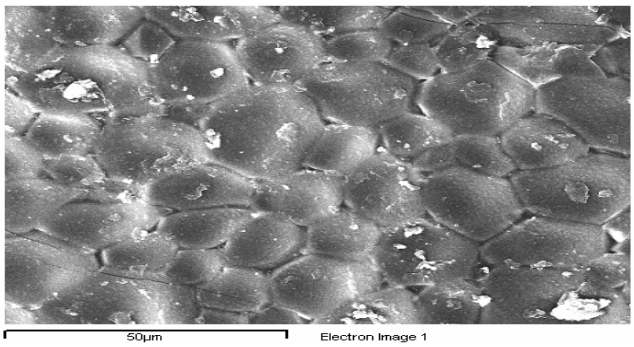

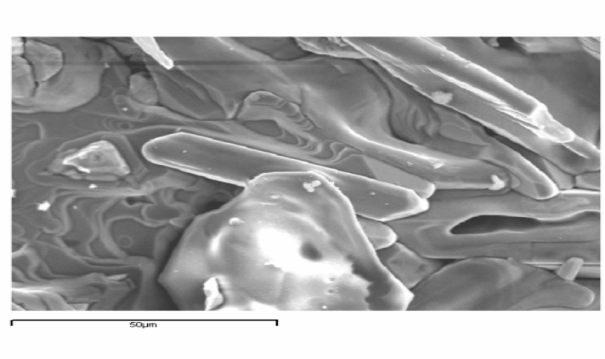

Sp2

Fig.II: SEM images of the spinels

An increase in barium is known to reduce the grain growth [12] while titanium enhances grain size [13] .Our spinels also follow this trend. SEM images show dense and well- defined grain formation in SP1.However the grain boundaries in SP2 are less defined. Compositional analysis of the spinels using the EDAX spectra shows that the stoichiometry is maintained in the powder. However, on the surface of the pellet **Fe > Ti > Ba** in SP1 whereas **Ba > Ti >Fe** in SP2 (Table II).

TABLE II COMPOSITIONAL ANALYSIS

Sample	**Surface**			**Stoichiometric composition**		
	Fe/Ti	**Fe/ Ba**	**Ba/ Ti**	**Fe/ Ti**	**Fe/ Ba**	**Ba /Ti**
SP1[12]	3.77	00	00	1.22	11	0.11
SP2[10]	0.71	1.2	0.603	1.9	4.33	0.43

In order to decide the cation distribution in a given sample, the intensities of diffraction from five spinel planes viz. (220), (311), (400), (440), (422) are taken into consideration [5]. The structure factor (F_{hkl}) relations for each plane/site are as mentioned below:

F_{220} = $8fa + 16fo (-1+ \cos 2\pi u)$

F_{311} = $4fa + 4fb + 32fo (\cos 6\pi u . \cos 2\pi u - \sin 6\pi u . \sin 2\pi u)$

F_{400} = $8fa – 16fb – 32fo (\cos 8\pi u)$

F_{422} = $8fa + 32fo (\cos 8\pi u . \cos 4\pi u)$

F_{440} = $8fa + 16fb + 32fo (\cos 8\pi u)$

Where fa, fb, fo are the scattering factors corresponding to the A (tetrahedral), B (octahedral) and oxygen sites respectively and u is the oxygen positional parameter.

The diffraction lines assigned to (311), (400) and (440) planes are attributed to both, the octahedral and tetrahedral sites. These intensities are independent of the cation distribution. The lines assigned to (220) and (422) are only due to tetrahedral sites and their intensities are influenced by the cation distribution.

The multiplicity (P) and Lorentz polarization factors (L_p) [24] along with the structure factors (using the above mentioned structure factor relations) are used in the formula; $I_{hkl}=|F_{hkl}|^2 P.L_p$ to determine their intensities [24]. The intensities are calculated for different cation distributions and the, coefficient of correlation (r) between the calculated and observed intensities are determined for each sample by the least square method. The results are reproduced by a solid line as a function of the Fe^{3+} content on the A site. In *Fig. III*, the results are confirmed by the Furuhashi method [5] and are also included in . Both these methods arrive at the same distribution; but the method of absolute intensities yields better results as the plot shows a decisive peak without any secondary maxima.

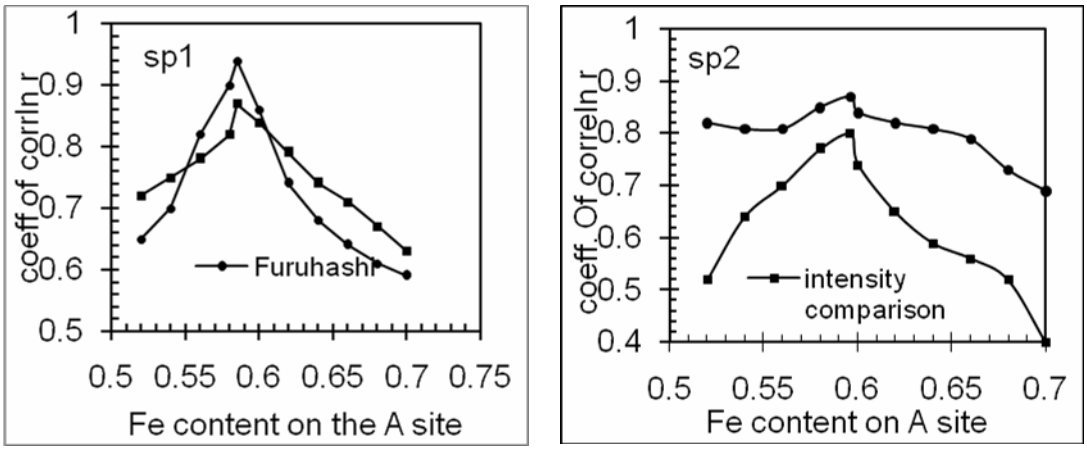

(Dotted line indicates Furuhashi method & solid line indicates the intensity comparison method)

Fig.III: The cation distribution as a function of Fe content on the A site

The best value of (r) is further improved upon by varying the oxygen parameter ´u' in steps. The best values of 'r' for SP1 and SP2 are 0.878 and 0.866 for u= 0.375 and 0.380 respectively. The relative percentage intensities calculated for the best values of r are compared with the observed ones in *Table III*. Also, the distribution of divalent, trivalent and tetravalent cations among the tetrahedral and octahedral sites in the two spinels is ascertained from the intensity ratios I_{220} / I_{440} , I_{220} / I_{400} , I_{220} / I_{311} , since these ratios are considered to be sensitive to the cation distribution and used extensively for the cation distribution [14], [9].

Table iii: relative percentage inten-sities; calculated {for the best r values} and observed

Hkl	SP1		SP2	
	Iobs	Ical	Iobs	Ical
220	46	34	69.2	44
311	100	100	100	100
400	17	55	28.5	38.3
422	13	44	-	-
440	45	59	49.4	57.5

Intensity Ratios are compared as in *Table IV*.

TABLE IV: INTENSITY RATIOS CORRESPONDING TO SP1 AND SP2

	I_{220} / I_{440}		I_{220} / I_{400}		I_{220} / I_{311}	
	Obs.	**Cal**	**Obs.**	**Cal**	**Obs.**	**Cal.**
SP1	1.02	0.57	2.7	0.62	0.46	0.34
SP2	1.40	0.76	2.4	1.15	0.7	0.44

The observed ratios exceed the theoretical values (*Table IV*). This only means that the calculated intensities need temperature factor and absorption factor corrections [15]. However they do not affect the cation distribution .The cation distribution is determined as:

$(Fe_{0.585}\ Ti_{0.335}\ Ba_{0.08})$ $[\ Fe_{\ 0.515}\ Ti_{0.565}\ Li_{0.9}\ Ba_{0.02}]\ O_4$ for SP1 and

$(Fe_{0.596}Ti_{0.104}\ Ba_{0.3})$ $[\ Fe_{\ 0.704}\ Ti_{0.596}\ Li_{\ 0.7}\ ]\ O_4$ for SP2.

It is interesting to note that Ba^{2+} prefers the tetrahedral sites. Lithium has been reported to prefer the B site [16]. Also, u >0.375 in SP2 indicates a distortion in the anion sublattice [17] which results in the small displacement of anions allowing expansion of the tetrahedral interstices. Therefore, it is thought interesting to determine interionic distances, radii of tetrahedral and octahedral interstices for which experimental values of lattice constants, oxygen parameter and radius of Oxygen ion=1.32A^0 are used [10]. The results are listed in *Table V*.

TABLE V: INTERIONIC DISTANCES CORRESPONDING TO SP1 & SP2

Inter-ionic distances (A^0)	**SP1**	**SP2**
Tetra-tetra A-A	3.6113	3.596
Tetra- octa. A-B	3.4576	3.443
Octa- octa B-B	2.9486	2.9362
Tetra-O separation A-O	1.8056	1.8700
Octa-O separation B-O	2.0850	2.0347
O-O tetra edge	2.9486	3.054
O-O shared octa edge	2.9475	2.8188
O-O unshared octa edge	2.9486	2.9374
Tetra radius	0.4857	0.5500
Octa radius	0.7650	0.7147

Interestingly, tetra-O separation, O-O tetra edge length and tetra radius are all larger in SP2. On the other hand, the octahedral radius is smaller in SP2 .This correlates very well with the tetrahedral

occupancy by Ba^{2+} having larger ionic radius. Further, the larger intensity corresponding to tetrahedral 220 plane of SP2 indicates that Ba^{2+} prefers it.

Dielectric Properties: The dielectric properties of polycrystalline ferrites arise mainly due to interfacial polarization and intrinsic electric dipole polarization [18]. The dielectric data of these spinels (*Table VI*) in the frequency range 10Khz-1Mhz. show a falling trend at room temperature. This is in agreement with Maxwell's Wagner model for interfacial polarization. The conductivity term is significant in both SP1 and SP2. SP2 displays the nature of a dielectric material in which conducting ellipsoids are surrounded by an insulating material [19]. This may be due to the higher concentration of Ba and Ti on the grain boundary as implied by the EDAX. The Cole-Cole plot (*Fig. IV*) also suggests a broadened relaxation frequency implying Ba and Ti rich grain boundary.

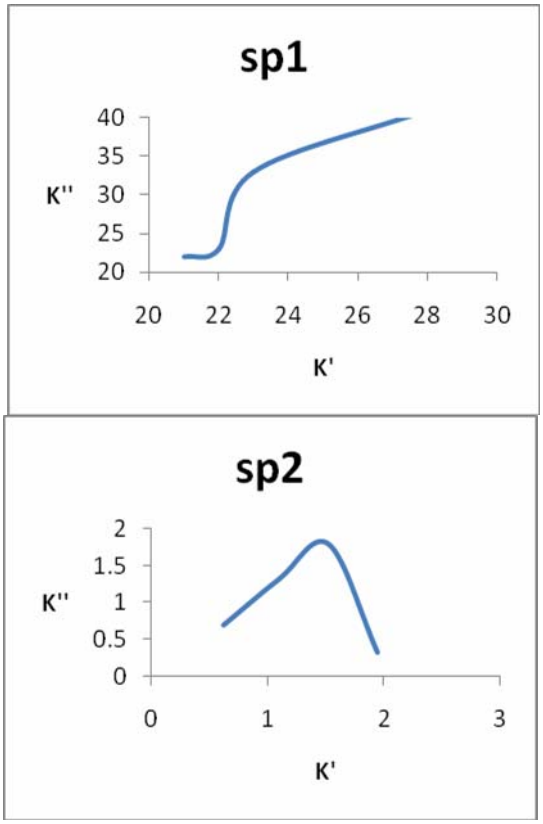

K' – Dielectric Constant, **K" – Dielectric Loss Factor**

Fig.IV: Cole Cole plots for the spinels

Ratios K'1000KHz/ K'100KHz , K'100KHz/ K'10KHz are <1.This indicates presence of space charge in both the spinels (*Table VII*). However, the space charge is much more in SP2. It is interesting to note that the dielectric constant at 1 Mhz. which gives contribution towards dipolar polarization is higher by several orders in SP2 vis-a vis SP1 as the barium content trebles. This implies that the presence of Ba

and Ti- rich grain boundary & tetragonality of SP2 appears to play a significant role in the enhancement of dipolar contribution as seen in $BaTiO_3$.

TABLE VI: DIELECTRIC CONSTANT AT ROOM TEMPERATURE

	SP1	**SP2**
K'1KHz	28	1.94 X10^4
K"1KHz	41	0.33 X10^4
K'10KHz	23	1.52 X10^4
K"10KHz	33	1.8 X10^4
K'100KHz	22	1.10 X10^4
K"100KHz	23	1.33 X10^4
K'1MHz	21	0.62 X10^4
K"1MHz	21.1	0.7 X10^4
Space Charge component (K'1KHz- K'1000KHz)	7	1.32 X10^4

Plots of dielectric constant versus absolute temperature at 1KHz. are shown in *Fig. V*. Both the samples show a slight decrease in dielectric constant initially from 300-400^o K. This is followed by a hysteresis loop which is characterized by its area and transition temperature.

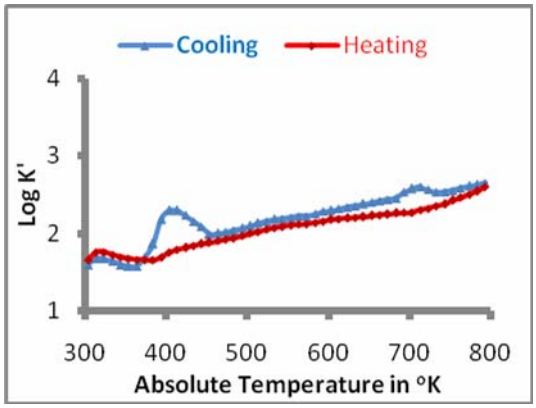

Sp1

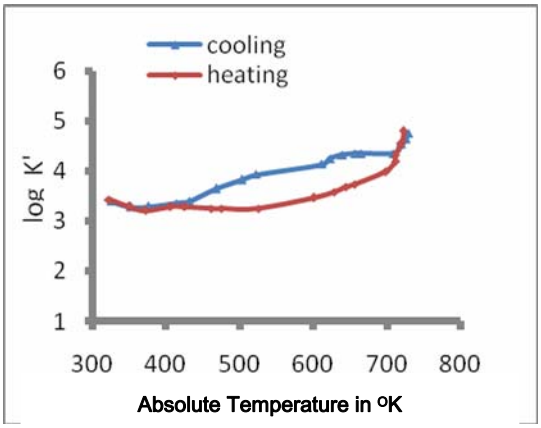

Sp2

Fig. V: Plots of dielectric constant V/s absolute temperature at 1KHz

Transport Properties: Room- temperature dc and ac resistivities of SP1 and SP2 are listed in *Table VII*. The smaller resistivities imply a significant presence of space-charge (interfacial polarization) in SP2. Such a significant difference between the two resistivities is likely to be due to the cation distribution , particularly on the octahedral sites [20]. The table indicates that the resistivity (ρ) increases with increasing Ti concentration.

TABLE VII: AC AND DC RESISTIVITY OF THE SPINELS

	ac Resistivity Ω.cm.	**dc resistivity. Ω.cm.**
SP1	855 x 10^3k.	11 x 10^3k.
SP2	0.54 x 10^3 k.	0.397x10^3 k.

The resistivity (ρ) is known to increase slightly for additive samples [21], [22], [23], [24], [25], [26]. In the present samples also, (ρ) increases with increasing Ti concentration. This may be explained as follows. According to the chemical formula of our investigated series, $Li_x Fe_{2-x} Ba_y Ti_{1-y}O_4$, as Ti concentration increases, the Fe-concentration decreases. Thus the probability of formation of Fe^{2+} ions and therefore the hopping between Fe^{2+} and Fe^{3+} decreases and the resistivity increases. Moreover, it is reported that the tetravalent ion is able to form stable bonds with Fe^{2+} ions [27]. Since Ti is tetravalent, it localizes Fe^{2+} ions that may be formed during sintering process. This localization hinders the Verwey-de Boer mechanism between Fe^{2+} and Fe^{3+} ions, resulting in an increase of the resistivity [27].

Plots of log resistivity vs. reciprocal of absolute temperature are investigated for activation energies as shown in *Fig. VI*.

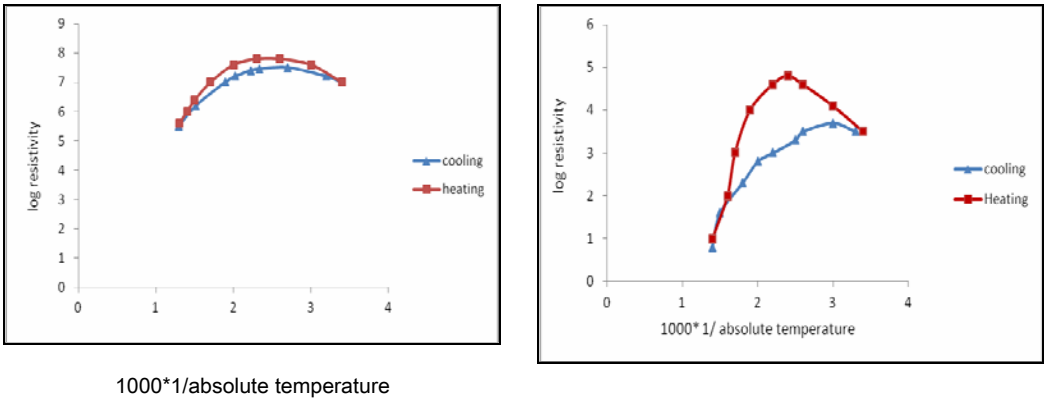

Fig.VI: Resistivity plots of spinels

The plot corresponding to SP2 shows a significant hysteresis effect. Both the curves exhibit a positive temperature coefficient region near room temp.; followed by a flatter extrinsic region and end with a linear intrinsic region. PTCR effect is not observed in pure $LiFe_5O_8$. The PTCR effect is more significant and activation energies are larger in SP2 (*Table VIII*). It is interesting to note that both the dielectric as well as transport hysteresis are observed at low frequency (1KHz) and are prominent only in the case of SP2 in the same temperature region from 350-700^0 K. Therefore, they may have arisen from the significant presence of interfacial polarization in SP2.

TABLE VIII: ACTIVATION ENERGIES (EV)

	ACTIVATION ENERGIES (eV)			Band Gap eV.
	Region1	Region2 (extrin.)	Region3 (intri.)	
	300-390K	390-530K	530-770K	
Sp1	PTC	0.2	0.60	1.2
Sp2	PTC.	0.27	1.048	2.096

The Band gap corresponding to SP2 is much larger than that to SP1.Band gap of pure $LiFe_5O_8$ is 1.6-1.8 eV [28].

Conclusion

Both the spinels fall in the $LiFe_5O_8$ space group namely Fd3m. The substitution with barium results in increased cell volume. Ba^{2+} preferentially enters the tetrahedral site. A new revised method to determine the cation distribution is reported. The EDAX establishes a Ba-Ti rich boundary when the presence of Ba^{2+} is substantial in the sample.

Both the interfacial and dipolar polarizations are observed to be considerably larger in SP2.Two relaxation frequencies 20KHz and 200KHz are observed in SP2. The resistivity measurements complement the presence of interfacial polarization. The bandgap corresponding to SP2 is very large and SP2 shows a colossal dielectric constant.

References

[1] Krupicka, S. and P.Novak. (1982) Ferromagnetic materials Ed. E.D. Wohfart (Amsterdam North Holland 3 194 .

[2] Landolt, Boerstein, (1970) Magnetic and other properties of oxides and related compounds. Vol. 3-4b, Springer Verlag, New York

[3] Smit, J. and H.P.J. Wijn. Ferrites, Philips, Eindhoran (1959).

[4] benjamin, L. and K.J .Button. Microwave Ferrites and Ferrites and Ferrimagnetes, Mctrraw Hill, New York (1962).

[5] Furuhashi, M. Inagali, S. Naka. J. In org. nucl.chem (1973), Vol.35 pp 3009-3014. pergamon Press.

[6] Grimes, N.W., (1975) Phys. Technol. 22.

[7] Galasso, F.S. in "Structure and Properties of Inorgani solids" (1970) Pergamm, Oxford p. 219.

[8] Camley, R.E., CE Patton, (1986) J of Mand MM, 54-57, 1601.

[9] porta P, Stone F S. and Turner R.G. (1974), J. Solid state Chemistry 11 135.

[10] Raul Valenzuela, (1994) Magnetic Ceramics, Cambridge University Press,.

[11] Postupolski, T., Prace. (1988). Inst. Tele. Radio Zesz, 107/871

[12] Chen, Laughlin,(1997) Ma. J. Appd Physi. 81, 4380

[13] Zhenringyue, Jizhou, Wang, (2003). Journal of European Ceramic Society, 23, 1, 189.

[14] Ohinishi, H. and Teranishi T (1961) J. Phys Soc., Japan. 16,36.

[15] Datta, R.K. and R. Roy . (1967) J .Am. Ceramic Society 50, 578

[16] White, Patlon, (1978) Magnetism and Magn. Materials, 9, 299 .

[17] Otero Arcan C, Rogrigeus Blanco, Fernandez MC (1990) J.Mater Sci. Lett. 9 229.

[18] Fortes, S.S., Duqua JGS and Macdo MA, (2006) Physica ,B. Cond. Matt, 384 88.

[19] Von Hipple, Dielectrics and Waves, John Wiley & Sons NY-(1954)

[20] Khanolkar Vrinda; (1990) Msc. (research) Thesis;

[21] Kim, H.T. and H.B. Im, (1982). Effects of Bi2O3 and Nb2O5 on the magnetic properties of Ni-Zn ferrites and lithium ferrites. IEEE Trans. on Magnetics, 18: 1541.

[22] Edelio, B., T.le Mercier and M. Quarton, (1995). J. Am. Ceram. Soc., 78: 365-368.

[23] Poltinnikov, S.A., (1966). Sov. Phys. Solid Stat., 8: 1144.

[24] Cullity, B.D., 1959. Elements of X-ray diffraction. Published by Addison-Wesley Publishing Company, Inc., Second Printing, pp: 330.

[25] Rezlescu, N. and E. Rezlescu, (1995) Phys. Stat. Sol. (a), 147: 553

[26] Rezlescu, N. and E. Rezlescu, (1996). Effects of addition of Na2O, Sb2O3, CaO and ZrO2 on the properties of lithium zinc ferrite. J. Am. Ceram. Soc., 79: 2105.

[27] Rana, C.P., J.S. Baijal and P. Kishan, (1983). J. Less- Common Metals, 165: 257.

[28] Dudley, G.J., Steele; (1978) J. Electro.Chem.Soc. 125, 1994.